High-efficiency Off-axis Coupling of Rotating Optical Signals Based on Internal Conical Reflection

Dagong Jia, [a,*] Fenjiao Yun,[a] Ruihang Wang,[a] Hongxia Zhang,[a] Tianhua Xu, [b] Tiegen Liu,[a]

[a]Tianjin University, College of Precision Instrument & Opto-electronics Engineering, Tianjin, China, 300072

[b]University of Warwick, School of Engineering, Coventry CV4 7AL, United Kingdom

*Corresponding author, E-mail: dagongjia@tju.edu,cn

Abstract. We propose an off-axis coupling method for rotating optical signals based on the internal conical reflection. An analytic model of off-axis coupling is developed and verified via simulation and experiment. According to theoretical analysis, the coupling efficiency depends on both the reflectivity of, and the number of reflections between, the conical and the circular plane mirrors. When the reflectivity of the conical and the circular plane mirrors are both constant, i.e. n=0.973, the coupling efficiency is decreased with an increase in number of reflections. Experimental results show good agreement with theoretical predictions. In addition, our experiment demonstrates that the proposed method can achieve a multi-channel signal coupling with a maximum insertion loss of 1.62dB in channel T1 and 0.98dB in channel T2.

Keywords: Optical fiber component; Off-axis coupling; Rotating optical signal; Internal conical reflection

1 Introduction

Off-axis fiber optic rotary joints (FORJs) provide an alternative solution to traditional on-axis devices when the central axis transmission channel is not available [1-5]. For instance, when the joint uses an on-axis “through-bore” to pass physical media such as gas, water, or oil, the light must be transmitted through the joint in an off-axis fashion [4-7]. Some radar systems, for example, use the central part of the rotation joint for high-pressure gas [7]. Off-axis transmission is also used in other applications such as computer topography, magnetic resonance imaging, marine propulsion systems, tank turrets, machine tools, and shipboard winches [5]. The key problem in

off-axis FORJs is the low efficiency signal coupling across the rotary interface. This paper studies ways to dramatically improve the efficiency of off-axis FORJs.

To date, many optical coupling methods have been proposed, all of which display various levels of transmission inefficiency. Coupling methods have traditionally fall into two categories: *direct* [8-12] and *reflective* coupling [13-16].

Directly coupled FORJs use one or four fiber collimators on the moving portion of the joint to emit an offset beam at a specific angle [8,11]. The stationary part of the joint holds several collimator receivers through which the emitted light is received. As the joint rotates, the emitter alternately aligns with different receivers. However, both the insertion loss and the fluctuation of the transmitted signal are large, which makes direct coupling unsuitable for many applications.

Reflective coupling, on the other hand, uses optical refractive and reflective elements to redirect the path of the light through the joint. Compared with direct coupling, reflective coupling reduces the signal power variation as the joint turns because refracted light is effectively available at all positions of the rotating joint.

An example of reflective coupling is that of M. Iverson [13] who employed a concentric annular mirror to reflectively propagate the optical signal within an annular mirror cavity. A large proportion of the incident energy was lost, however, when the beam was projected into and propagated within the mirror. As a result, coupling efficiencies were low. Snow *et al*. proposed an annular optical waveguide that restricts the optical path of the signal in which the optical signals can be restrictively transmitted [2]. In this way, off-axis signals are coupled across the rotary interface. Although the waveguide is compact and simple, the total coupling efficiency is still low, having an insertion loss more than 40 dB when an acrylic waveguide is used. The dynamic variation of optical power, namely, the variation of insertion loss during rotation, is 6-10dB. Recently, H. Zhang *et al*. employed conventional optical components, mirrors, prisms, etc., to make a low-loss off-axis FORJ [14]. The coupling system, however, is difficult to assemble and align due to the complex structure and the optical path. J. Ding *et al*. proposed another low-loss method, a reflective approach wherein they installed infrared right-angle prisms between optical fiber collimators to deflect off-axis light [15,16]. Experimental results, however, showed that the insertion loss was still substantial, about 22dB, with coupling variation of 4.33 dB [15]. Such large loss and coupling variation limits the practical applications of this technique. In fact, none of the

reported off-axis methods have been successfully applied due to their high insertion loss. Therefore, it is imperative to study approaches that enhance the coupling efficiency of FORJs.

In this paper, we propose and experimentally demonstrate an off-axis coupling method of rotating optical signals based on the internal reflection of conical mirror. The rest of paper is organized as follows. Theoretical model is developed in Section 2. Simulation and experimental results of the off-axis FORJ are discussed in Section 3. Conclusion is drawn in Section 4.

2 Theoretical Analysis

Fig. 1 shows the schematic of the light internal reflection in a conical mirror. A light travel from the source point C to the reflection point A located on the conical mirror and is then reflected towards spatial point B. The cylindrical coordinates of points A, B and C are listed as follows: A:(R, θ_0, Z), B:(R_2, θ_2, Z_2), C:(R_1, θ_1, Z_1). The unit normal vector at point A is set as $\vec{n}$ =(cos$\theta_0$cosβ_0, sin$\theta_0$cosβ_0, sinβ_0), where β_0 is the half cone angle of the conical mirror. H_1 is the height of the conical mirror.

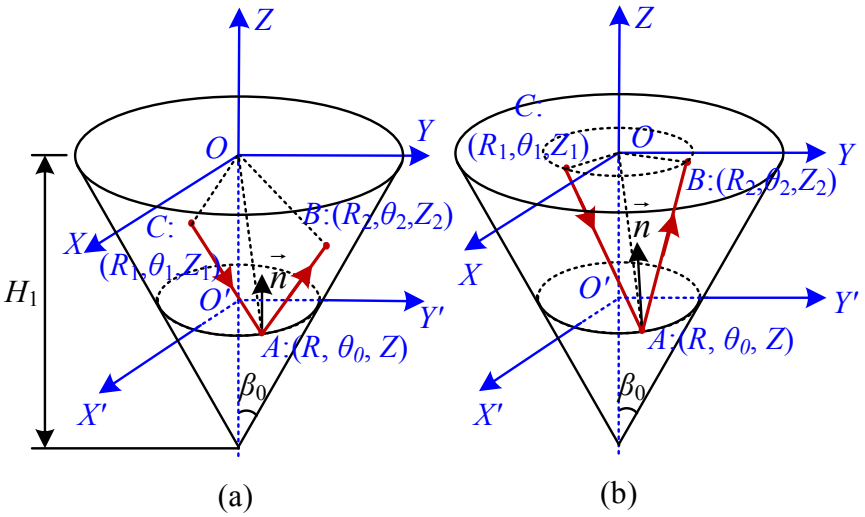

Fig. 1 Schematic diagram of conical mirror reflection, (a) $Z_1 \neq Z_2$ and $R_2 \neq R_1$ (b) $Z_1 = Z_2$ and $R_2 = R_1$.

Since reflected and incident angles are equal, the following equation is obtained:

$$\frac{\overrightarrow{AC}\cdot\vec{n}}{|AC|}=\frac{\overrightarrow{AB}\cdot\vec{n}}{|AB|}. \tag{1}$$

According to Fermat's principle [17,18], the total length of the ray path L is minimized, then we have:

$$\frac{\partial L}{\partial \theta_0} = 0 \text{ and } \frac{\partial L}{\partial Z} = 0, \tag{2}$$

$$L = |CA| + |AB|. \tag{3}$$

In Fig.1 (b), if point C and point B are on the same circumference, we obtain from Eqs. (1--3) the following:

$$R_1 R_2 \sin(\theta_1 + \theta_2 - 2\theta_0) + R_2(Z_1 - H_1)\sin(\theta_2 - \theta_0)\tan\beta_0 + R_1(Z_2 - H_1)\sin(\theta_1 - \theta_0)\tan\beta_0 = 0, \tag{4}$$

$$\begin{aligned}&[R_1\cos(\theta_1 - \theta_0) + (Z_1 - H_1)\tan\beta_0][(Z - Z_2) + (Z - H_1)\tan^2\beta_0 + R_2\tan\beta_0\cos(\theta_2 - \theta_0)] + \\ &[R_2\cos(\theta_2 - \theta_0) + (Z_2 - H_1)\tan\beta_0][(Z - Z_1) + (Z - H_1)\tan^2\beta_0 + R_1\tan\beta_0\cos(\theta_1 - \theta_0)] = 0\end{aligned}, \tag{5}$$

where

$$R_1 = R_2 \text{ and } Z_1 = Z_2. \tag{6}$$

According to the geometric relationship in Fig.1 (b), we can also derive,

$$R = (H_1 - |Z|)\tan\beta_0. \tag{7}$$

From above analysis, we establish a theoretical model for the off-axis coupling of rotating optical signals using the internal reflection principle of conical mirrors. Figure 2 shows the proposed theoretical model in which the optical signals are transmitted in an offset manner against the rotary axis in the conical mirror. The theoretical model is a modified cylinder whose upper surface is a circular plane mirror with radius r and the lower surface is a conical mirror. The center of the modified cylinder is a cylindrical hole with a radius of r_0. In Fig.2, a beam from optical collimator A is sent into the conical mirror, and another optical collimator B, used as the receiver, is located on the exit window of conical mirror. The green line represents the path of the optical signal where A, B and C are reflection points which are located on the upper circular plane mirror and points A', B' and C' are reflection points located on the lower conical mirror. The points A, B and C determine circle 1 and points A', B' and C' determine circle 2. When coupling rotating optical signals, the circular plane mirror rotates about the z-axis, and circle 1 is the trace of the incident light. From Fig. 2(a), we note that circle 2 with radius r_2 is the intersection of the plane $X'O'Y'$ with the conical mirror. Circle 1 and circle 2 are parallel to each other, and the relative height is $h = r_1\sin\theta\tan\theta\tan\beta$, where $r_1 = r_2\cos\theta$. The exit window is located on circle 2. The optical signal can propagate between circle 1 and circle 2 in a reflective manner. We also note that the transmitted optical beam is perpendicular to the radial direction of the reflection point on circle 1 (like e.g., point A in Fig. 2 (a)). Fig. 2(b) shows the trace of optical coupling for the transmission of one

optical signal. Point B_1 is the projection of point B onto plane $X'O'Y'$. Thus we obtain $O'B_1 \perp A'B'$ and $BB_1 \perp OB$, from which we get $OB \perp A'B$ and $OB \perp BB'$.

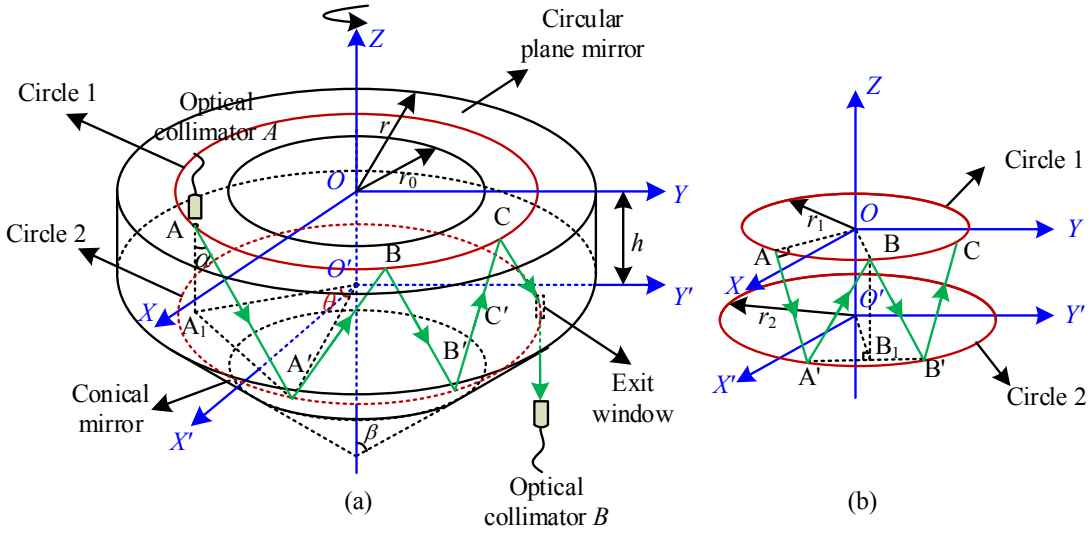

Fig. 2 (a)Theoretical model of the off-axis coupling of rotating optical signal, (b) The manner of optical coupling for one incident optical signal. (Circle 1 is the motion track of the input optical beam and circle 2 is the stationary track of optical beam reflection)

Point A_1 on the plane $X'O'Y'$ is the projection of point A (see Fig. 2(a)). According to the geometrical relationship, the propagation equation of the light in the theoretical model can be expressed as:

$$\theta = 2\pi / N, \tag{8}$$

$$\sin\theta \tan\beta \tan\alpha = 1, \tag{9}$$

where θ is the deflection angle of the optical signal in the horizontal direction, α is the incident angle, and β is the half cone angle of conical mirror. N is the number of reflections.

According to Eq. (9), we obtain a function of θ against N, as shown in Fig.3. It can be seen that θ falls with increasing N.

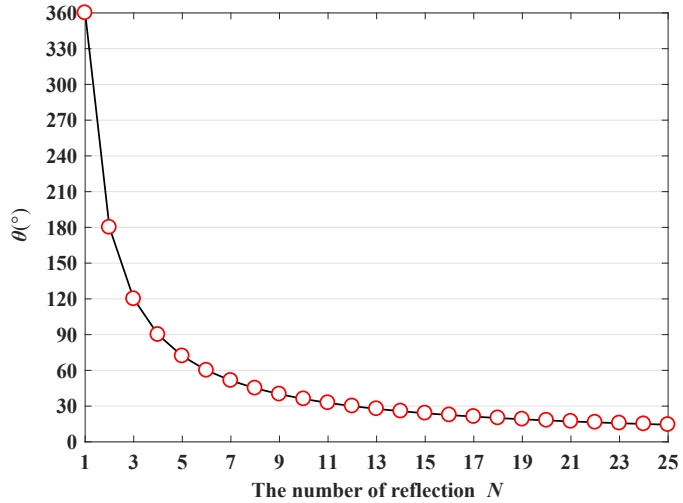

Fig.3 The function of θ against N

When θ=15.65°, we can draw the function of α and β according to Eq. (10), as shown in Fig.4. As illustrated in Fig. 4, α falls with increase of β.

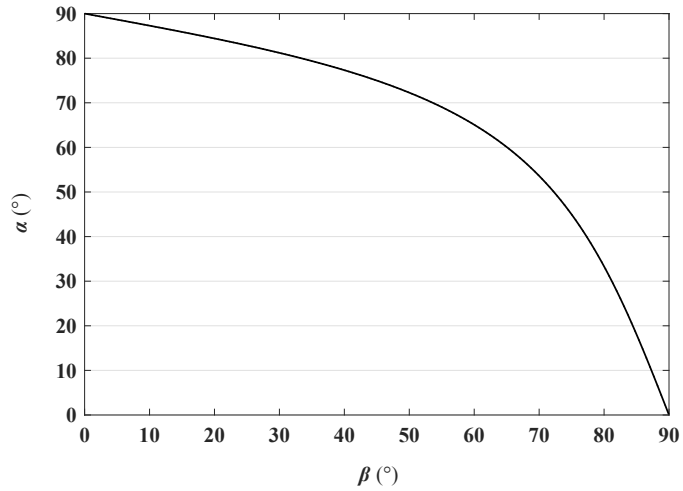

Fig.4 The function of β against α

Fig. 5 is a front view of multi-channel theoretical model. As illustrated in Fig. 5, the height of the theoretical model and modified cylinder is $\boldsymbol{H}$ and h_0, respectively. According to the geometric relationship, the following equation can be derived:

$$r = (r_2 + 1)\sin^2\theta\tan^2\beta - h_0\tan\beta\,, \tag{10}$$

$$H = r_2 \sin^2\theta \tan^2\beta + \frac{r_2}{\tan\beta} - \frac{r_0}{\tan\beta}. \tag{11}$$

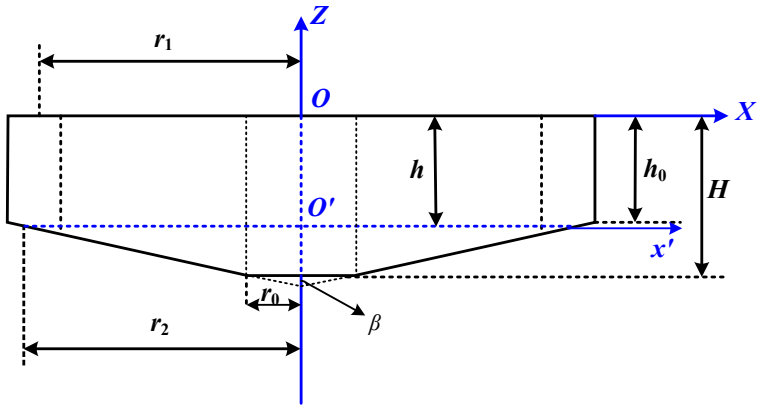

Fig. 5 Front view of theoretical model

Suppose h_0=5mm, r_0=15mm and r_2=35mm. According to Eqs. 10, 11 when θ=15.65°, we can plot functions of r against β, and H against β, as shown in Fig.6 and Fig.7, respectively.

Fig. 6 shows the function of H against β. According to Fig. 6, we find that H first falls and then rises with increasing β.

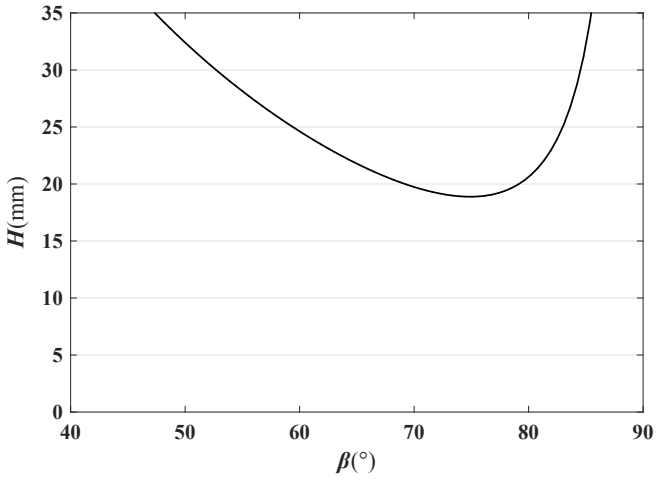

Fig. 6 The function of H against β

Fig. 7 shows the function of r against β. According to Fig. 7, we see that r first falls and then rises with increasing β.

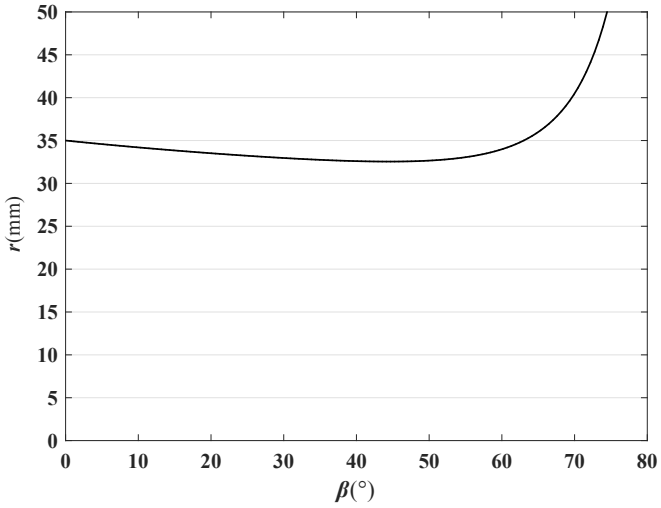

Fig. 7 The function of r against β

.

3 Model Establishment and Simulation

Since Circles 1 and 2 are considered as the trace of optical signal propagation, the two circles determine a transmission channel, T1. Based on the above analysis, we determine the parameters of channel T1 to be as follows: r_1=33.7mm, r_2=35mm, β=70°, h_0=5mm, r_0=15mm, θ=15.65°, r= 40.49mm, H =19.74mm, α=53.46°.

Suppose the reflectivity of the conical mirror and circular plane mirror is n, and the input power of the optical signal is P_{IN}. The output power P_{OUT} is then given by:

$$P_{OUT}=P_{IN}\times n^{N}. \tag{12}$$

The insertion loss (IL) is given by:

$$IL=-10\lg\frac{P_{OUT}}{P_{IN}}=-10\lg n^{N}. \tag{13}$$

Eq. (13) shows that the insertion loss is related to both the reflectivity of, and the number of reflections between, the conical and the circular plane mirrors. IL scales with the decrease of reflectivity, or the increase of the number of reflections.

The coupling efficiency (CE) is defined as:

$$CE=P_{OUT}/P_{IN}=n^{N}. \tag{14}$$

Eq. (14) shows that the coupling efficiency increases with increasing reflectivity and decreases with the number of reflections.

Fig. 8 is the schematic of optical signal propagation along channel T1. From Eq. (13) and (14), we find that the insertion loss or coupling efficiency scales with both the reflectivity of, and the number of reflections between, the conical and the circular plane mirrors. To achieve high coupling efficiency or, equivalently, less insertion loss, we design two exit windows, *A* and *B,* at fixed positions on circle 2. The central angle of the exit windows *A* and *B* is 2θ=31.3°, and the angle between the exit windows is 140.04°. When the rotating optical signal reflectively propagates along channel T1, it reflects N_{T1} times before leaving channel T1 from the exit window *A* or *B*, where N_{T1} is an even number ($0 \le N_{T1} \le 10$). For example, if the optical signal is perpendicularly incident at point *A* and is coupled along channel T1, then it can reflect 4 times before leaving the channel from exit window *A*. Suppose we only design one exit window, *B,* at fixed positions on circle 2. The input optical signal will be reflected 14 times before leaving channel T1 from exit window *B*, resulting in a low coupling efficiency. Fig. 12 is the theoretical relationship between the coupling efficiency and the number of reflections when n=0.973. From Fig. 12, we find that the coupling efficiency decreases with increasing N_{T1}. When N_{T1} is in {0, 2, 4, 6, 8, 10}, the theoretical value of coupling efficiency is 100%, 95%, 89%, 85%, 80% and 76%, respectively.

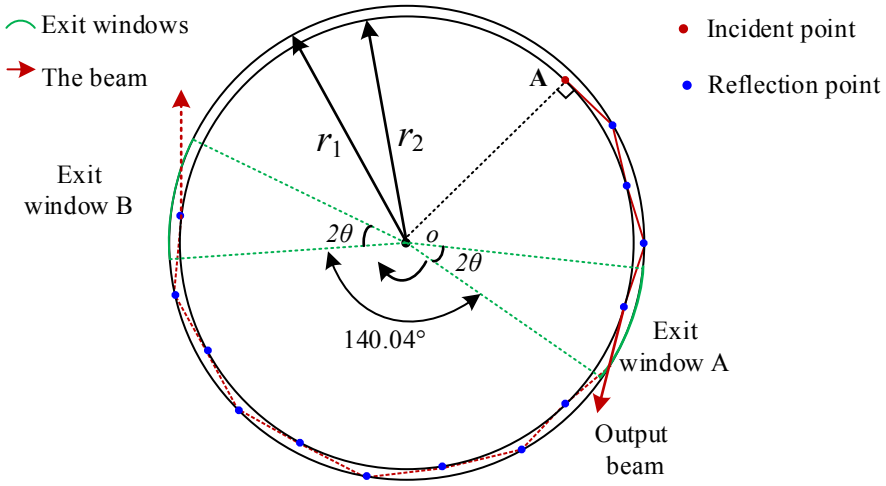

Fig. 8 The top view of optical signal coupling along channel T1

For the purpose of multi-channel signal transmission, similar to channel T1, we add another transmission channel, T2, that consists of circle 1' with radius r_1' and circle 2' with radius r_2'. In channel T2, the deflection angle of the optical signal in the horizontal direction is θ' and the

incident angle is α'. To eliminate the crosstalk between the two channels during off-axis coupling, the condition $r_2>r_2'$ has to be satisfied. When θ'=18.95°, according to Eq. (9--11), we determine the parameters of a channel T2 to be as follows: r_1'=28.56m, r_2'=30.19mm, α'=48.26°. We design two exit windows A' and B' at fixed positions of the circle 2'. The central angle of the exit windows A' and B' is $2\theta'$=37.9°, and the angle between exit window A' and B' is 132.65°. When the rotating optical signal reflectively propagates along channel T2, it reflects N_{T2} times before leaving channel T1 from the exit window A' or B', where N_{T2} is an even number ($0\leq N_{T2}\leq 8$).

In order to verify the proposed theoretical model, we carried out numerical simulations. First, a 3D model was constructed as shown in Fig. 9. There, the annular plane mirror is the rotor in the off-axis coupling system, and the combination of the conical mirror and the cylindrical through-hole is the stator. These constitute a two-channel off-axis rotary joint where the annular plane mirror rotates around a central axis (of rotation). Fig. 10 shows the optical propagation along the transmission channel within the 3D model using ray tracing software.

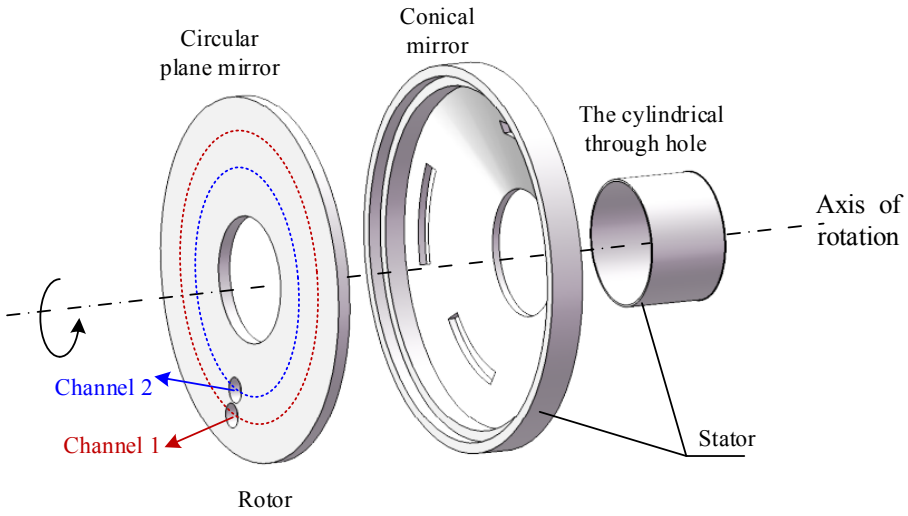

Fig. 9 The 3D model of off-axis rotating optical signal coupling

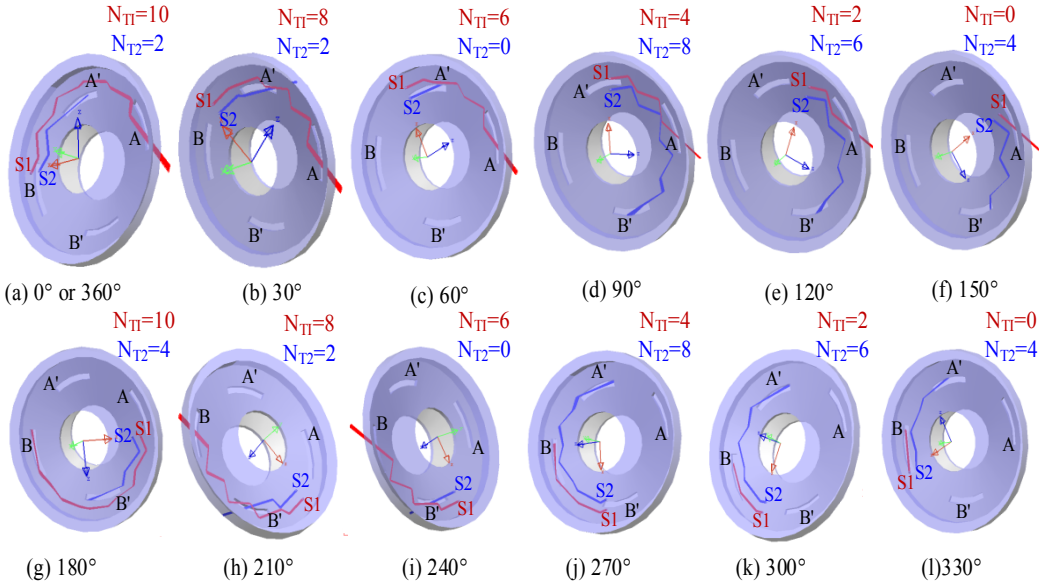

Fig. 10 Ray tracing of the transmission channel within the 3D model

As shown in Figs. 10(a-l), the beams are reflectively transmitted along channels T1 and T2 when the plane mirror rotates around the central axis. In the simulation, the rotation angle varies from 0° to 360° in 30° increments. In channel T1, the beam S1 is reflected N_{T1} times before exiting windows *A* or *B*, where N_{T1} is an even number ($0 \le N_{T1} \le 10$). Similarly, in T2, the beam S2 is reflected N_{T2} times before exiting windows *A*' or *B*' where N_{T2} is an even number ($0 \le N_{T2} \le 8$). From the results, we observed no crosstalk between T1 and T2 during transmission. Simulation results achieved good agreement with the theoretical model, and indicated that the proposed coupling method can realize off-axis optical signal transmission.

4 Experiment and Discussion

To further verify the theoretical model, we set up an experimental testbed and measured the coupling efficiency and the variation of insertion loss.

Fig. 11 shows the experimental setup. It consists of a 1550nm laser diode light source, a high-precision 5-axis stage, V-mounts, a single-mode optical fiber collimator (1550nm), and a power meter. The optical signals are fed into the off-axis coupling system using the collimator. The direction is determined to a resolution of 2um by the 5-axis stage. The output power of the light source is -9.09dBm measured by Optical Power and Energy Meter of model PM100D. The measured reflectivity of both the conical and plane mirrors is 0.973. During the experiment, we measured both the coupling efficiency for different values of *N* and the variation of insertion loss during mirror rotation

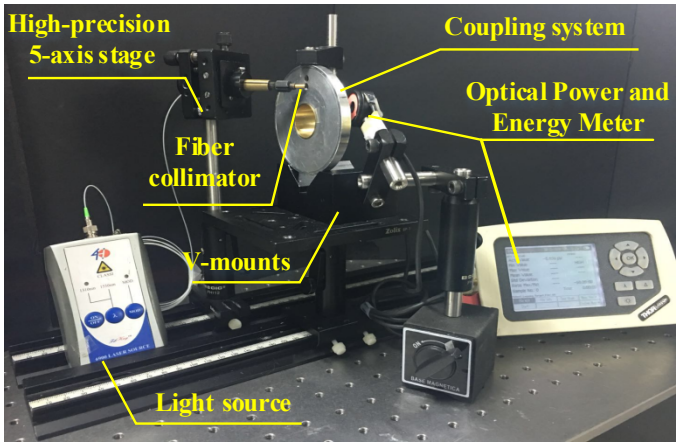

Fig. 11 Experimental setup of measurement of coupling

Fig. 12 shows the coupling efficiency of channels T1 and T2 for different number of reflection. It can be seen that the coupling efficiency decreases with increasing number of reflection. In channel T1, when the number of reflection is 0, 2, 4, 6, 8 or 10, the experimental value of coupling efficiency is 99.5%, 94.58%, 89.16%, 83.12%, 82.36% and 68.53%, respectively. Similarly, in channel T2, when the number of reflection is 0, 2, 4, 6 and 8, the experimental value of coupling efficiency respectively is 99.51%, 94.42%, 91.83%, 84.55% and 80.18%, respectively. The coupling efficiency of channel T1 is more than 68.5% and the minimum coupling efficiency of channel T2 is 80%. The main reason that the coupling efficiency is lower in channel T1 than T2 is that the number of reflections in T1 is larger than in T2. Experimental results are in good agreement with theoretical predictions when n=0.973. the small discrepancies between theoretical and experiment results are due to machine error and small reflectivity variations in the mirrors when N =10.

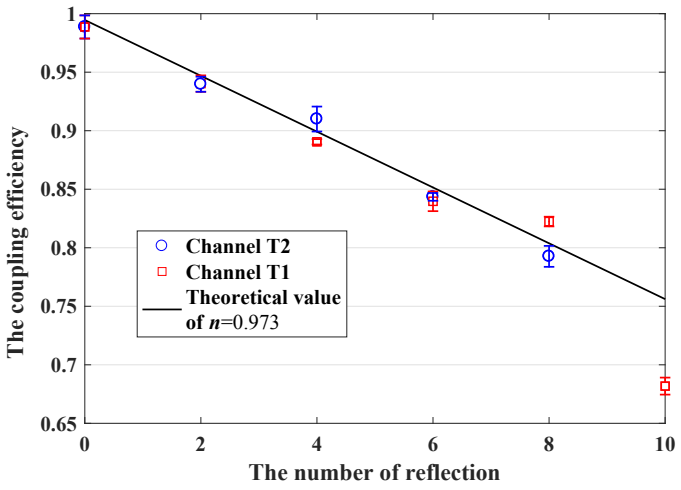

Fig. 12 The coupling efficiency of channels T1 and T2 for different number of reflection

Since the insertion loss is a key indicator for FORJ, the insertion loss of channel T1 and channel T2 are measured at different rotation angles. The measurement results are shown in Fig. 13. In channel T1, the maximum insertion loss is 1.62dB and minimum insertion loss is 0.02dB. Insertion loss rotating variation (another parameter of performance) is calculated to be 1.6dB. In channel T2, the maximum insertion loss is 0.98dB and minimum insertion loss is 0.03dB. Insertion loss rotating variation is calculated to be 0.95dB. The main reason that the insertion loss (or insertion loss rotating variation) is lower in channel T2 than T1 is that the number of reflections in T1 is larger than in T2. In addition, we can also find from Fig. 13 that insertion loss rotating variation is the same as the maximum insertion loss. It indicates that the rotation variation of insertion loss is larger. Compared to the coupling methods reported in Refs. [2], [11], [12] and [15], the proposed coupling approach is effective and can achieve a considerably lower insertion loss. The experimental results are in good agreement with predictions when n=0.973.

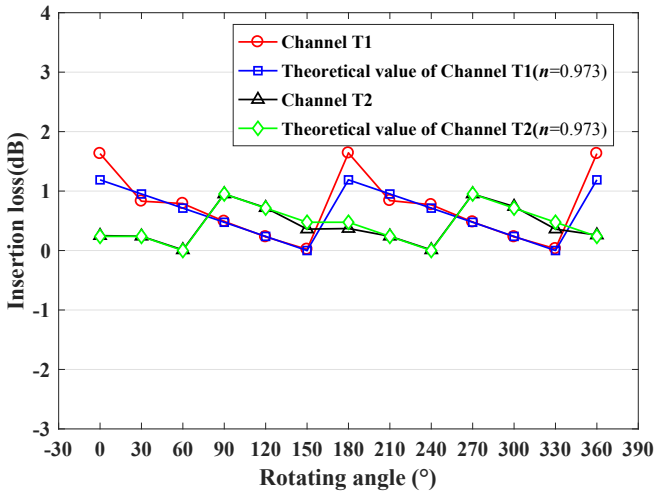

Fig. 13 The insertion loss of channels T1 and T2 for different rotation angles.

5 Conclusion

The internal reflection of conical mirror is an effective way to transmit off-axis optical signals. Based on the internal reflection of conical mirror, we proposed and demonstrated a coupling method to transmit off-axis optical signals across a rotary interface. Experimental results show that this off-axis coupling structure can achieve a high-performance multi-channel signal transmission. The proposed coupling method has a significantly lower insertion loss compared to conventional methods [2,11,12,15]. The issue of large rotation variation of insertion loss, which exists in all current off-axis FORJs [2,11,12,15], is still an open problem to research. Future work will incorporate investigating the reduction of the variation of the insertion loss in this proposed approach.

Acknowledgments

This work was partially supported by the Project of the National Natural Science Foundation of China (Grant No. 61875152 and U1813207).

References

[1] D. G. Jia et al., "Research Progress on Off-axis Fiber Optic Rotary Joint," *Acta*. *Armam*. 34(11),1454-1460 (2013).
[doi:10.3969/j.issn.1000-1093.2013.11.018]

[2] J. W. Snow et al., "Off-axis optical rotary joint," US patent 5,297, 225, Mar 22,1994.

[3] D. G. Jia et al., "Bidirectional dynamic data transmission through a rotary interface," *Opt*. *Eng*. 44(5), 050503 (2005).
[doi:10.1117/1.1906235]

[4] R. F. Mckay, "Off-axis rotary joint," US patent 7,372,230, May 13, 2008.

[5] H. Zhang et al., "Through-bore fiber optic slipring," US patent 8,554,029, Oct 8, 2013.

[6] H. Zhang et al., "De-rotating mechanism for off-axis fiber optic rotary joint," US patent 9,927,579, Mar 27, 2018.

[7] F. Liu et al, "Design and Implementation of an Off-Axis Rotary Optical Fiber Transmission System," *Chin. J. Las*. *42*(9), 156-162 (2015).
[doi: 10.3788/CJL201542.0905001]

[8] T. Mercey et al., "Rotating optical joint," US patent 6,898,346, May 24, 2005.

[9] Z. H. Lu, et al., "A kind of hollow optical fiber rotation connector," *Mod*. *Tran*. 2, 71-74 (2017).
[doi:10.3969/j.issn.1673-5137.2017.02.004]

[10] W. W. Koch et al., "Proof-of-concept model of a multichannel off-axis passive bidirectional fiber optic rotary joint," *Proc. SPIE*. 0931, 94-98 (1988).
[doi: 10.1117/12.946652]

[11] Y. Ying et al., "Design and experiment of an off-axis fiber-optic rotary joint," *Opt. Tech*. 39(2):188-192 (2013).
[doi:10.13741/j.cnki.11-1879/o4.2013.02.016]

[12] Q. X. Zheng et al., "Design and implementation of an off-axis rotary optical communication system," *J. Optoe. Laser.* 23(12):2310-2315 (2012).
[doi: 10.16136/j.joel.2012.12.022]

[13] M. L. Iverson, "Optical sliprings," US patent 4,109,997, Aug 29, 1978.

[14] H. Zhang et al., "Off-axis fiber optic slip ring," US patent 7,792,400, Sep 7, 2010.

[15] J. Ding et al., "Design and realization of the off-axis fiber optic rotary joint with large inner diameter," *J. Optoe. Laser.* 24(11), 2075-2080 (2013).
[doi: 10.16136/j.joel.2013.11.003]

[16] X. H. Wang et al., "Loss Characteristics Analysis and Optimization of an Off-Axis Rotary Optical Fiber Communication System,". *Appl. Mech. Mater. 596*, 788-793 (2014),
[doi: 10.4028/www.scientific.net/AMM.596.788]

[17] Y. Zhang et al, "MPI Based Parallel UTD with Analytical Methods to Determine Reflection Points on Cylinders and Cones," *J. Electromagn. Waves. Appl.* 19(3), 355-371 (2005).
[doi: 10.1163/1569393054139651]

[18] N. Wang et al., "Study on reflection ray-tracing method of UTD based on NURBS modeling," *Proceedings of APMC Conference* on *Microwave*, IEEE, 2005.
[doi:10.1109/APMC.2005.1606659]